Structure and corrosion properties of stainless steel after high-power ion beam processing

Structure and corrosion properties of stainless steel after high-power ion beam processing

M V Zhidkov*, M Y Gazizova[1], A E Ligachev[2], S K Pavlov[3] and G E Remnev[3]

[1]Belgorod State National Research University, 85 Pobedy Str., 308015, Belgorod, Russia
[2]Prokhorov General Physics Institute of the Russian Academy of Sciences, 38 Vavilova St., 119991 Moscow, Russia
[3]Tomsk Polytechnic University, 30 Lenina St., 634050 Tomsk, Russia

*Corresponding author: zhidkov@bsu.edu.ru

Abstract. In this study, the surfaces of AISI 321 stainless steel samples were irradiated with one shot of a high-power ion beam (HPIB) at pulse energy densities of 1 and 3 J/cm^2. The surface morphology and structural-phase state in the near-surface layers of the treated samples were analyzed using scanning electron microscopy and electron backscatter diffraction. Additionally, the influence of HPIB processing on the resistance to intergranular corrosion was investigated using electrochemical experiments.

1. Introduction

High-power ion beam (HPIB) processing is one of the promising methods used for the surface modification of metallic materials. The high-energy impact of powerful ion beams with an intensity of 10^7 W/cm^2 and more can be accompanied by a number of processes, such as heating, melting and evaporation, excitation of compression waves in the target because of the recoil pulse and rapid cooling of the heated surface layer of the target at a rate of 10^9-10^{10} K/s [1]. These processes lead to structural-phase transformations and changes in the surface topography of materials. Moreover, materials exposed to HPIB exhibit appreciable surface properties, such as resistance to wear and corrosion, microhardness, and fatigue strength [2-4].

The main features of the formation of craters on high-speed steel surfaces after ion irradiation have been extensively studied [5, 6]. Additionally, another study investigated the topography and properties of 316L stainless steel after HPIB processing [7].

In this study, we elucidated the topographical and structural changes in AISI 321 stainless steel irradiated by a HPIB and investigated its subsequent susceptibility to intergranular corrosion.

2. Experimental details

AISI 321 stainless steel (Fe–0.12C–18Cr–10Ni–0.5Ti) was used in our experiments after warm rolling (ε = ~1, T = 400 °C). This material was prepared in the form of rectangular slabs, and its surfaces were mechanically polished using a rotary polishing machine LaboPol-5 (Struers). Ion irradiation of the samples was performed using a TEMP-4M pulse accelerator [8]. The composition of the ion beam was as follows: carbon ions (C^+, C^{n+}) and protons (H^+) at a ratio of 85:15. The accelerating voltage was 250

kV, and the pulse duration (at half maximum of the accelerating voltage) was 100 ns. The residual pressure in the chamber was 2×10^{-2} Pa. The pulse energy densities (F) were 1 and 3 J/cm^2.

The structure and topography of the ion-beam-processed surface were studied using a scanning electron microscope (SEM, FEI Quanta 600) equipped with energy dispersive spectrometry (EDX, resolution: 0.2.–0.25%) and electron backscatter diffraction (EBSD).

Electrochemical experiments were performed using an IPC-Pro potentiostat and a standard three-electrode system. Silver chloride was used as the reference electrode with a carbon counter electrode. The corrosion resistance was examined in a solution of 0.01 mol/L KSCN and 0.5 mol/L H_2SO_4 using the double loop electrochemical potentiodynamic reactivation (DL-EPR) method at 30 °C.

3. Results and discussion

3.1. Surface topography

Figure 1 illustrates the SEM images of the irradiated stainless steel surfaces at different values of F. Rounded craters with concave centers were formed on the steel surfaces after ion beam processing. Craters were uniformly distributed over the sample surface. The average crater size was approximately 20 μm for F = 1 J/cm^2, and increased to 25 μm for F = 3 J/cm^2. The surface density of the craters increased from 2.7 x 10^4 to 4 x 10^4.

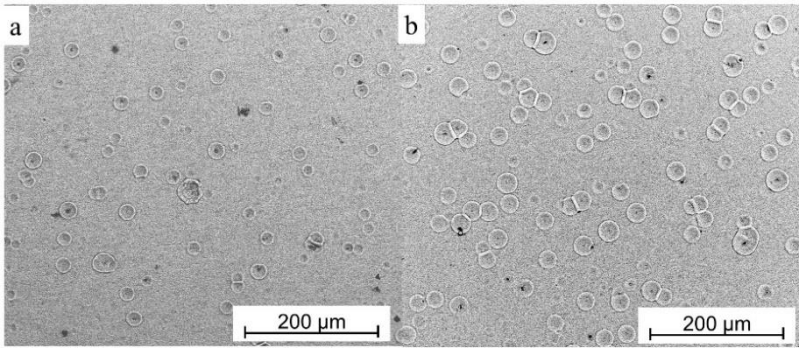

Figure 1. Top-view topography of the surface of samples of AISI 321 steel irradiated by HPIB at F=1 J/cm^2 (a) and F=3 J/cm^2 (b).

Figure 2 illustrates the EDX maps of the craters on the irradiated surface of AISI 321 stainless steel. Figure 2 (b) corresponds to the map distribution of chemical elements: Ti, S, Fe, Cr, Ni. In our experiments, the centers of the craters were rich in Ti and S, but poor in Ni, Cr and Fe. Craters appear to be formed on the inclusions of TiS or $Ti_4C_2S_2$ [9] that were present in the steel prior to processing.

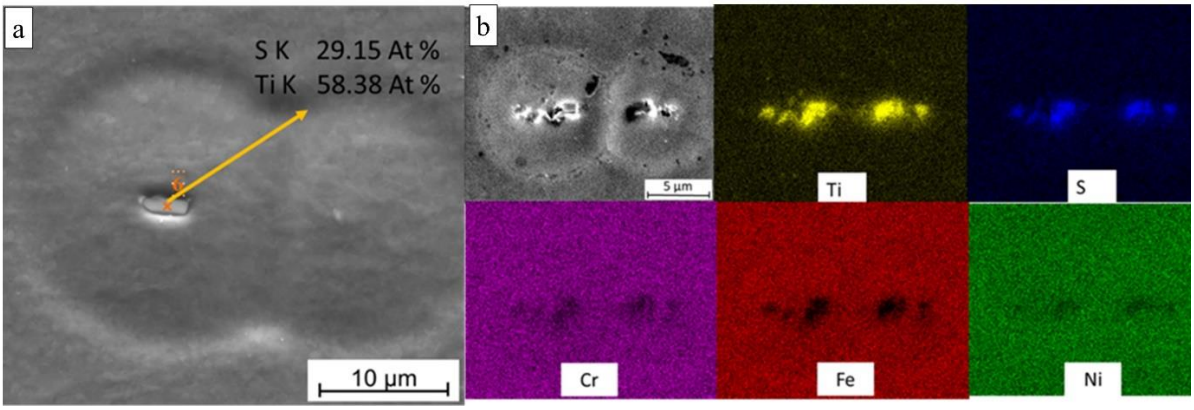

Figure 2. SEM image (a) and EDX maps (b) of the crater of AISI 321 stainless steel surface irradiated by HPIB.

The mechanism of crater formation has been proposed [5]. If the energy density exceeds the ablation threshold, the inclusions vaporize prior to matrix. Local ablation and eruption induced by partial vaporization drive the melt flow, leading to the formation of craters [5]. In [6], it was reported that the inclusion can also generate a crater during ion processing, despite the lack of vaporization of the inclusions on the target surface [6]. In this case, the difference in surface tension between the molten inclusion and the matrix can drive the melt to flow, generating a crater on the molten target surface [6].

3.2. Structure and phase composition of the near-surface layers

Figure 3 illustrates the structure of the steel surface before and after ion beam processing. In the initial state, the steel has a fiber-like structure with a mean grain size of approximately 500 nm and an axial inequality coefficient of approximately 5. The share of high-angle grain boundaries (HAGBs) was 57%. The ion irradiation altered the near-surface layer structure. The steel near-surface layers obtained at F = 1 J/cm^2 consist of a structure close to the equiaxed ultrafine-grains, with an average grain size of ~450 nm. In this case, the share of HAGB increased to 90%. Meanwhile, after irradiation with F = 3 J/cm^2, the average grain size increased to 600 nm (Figure 3c).

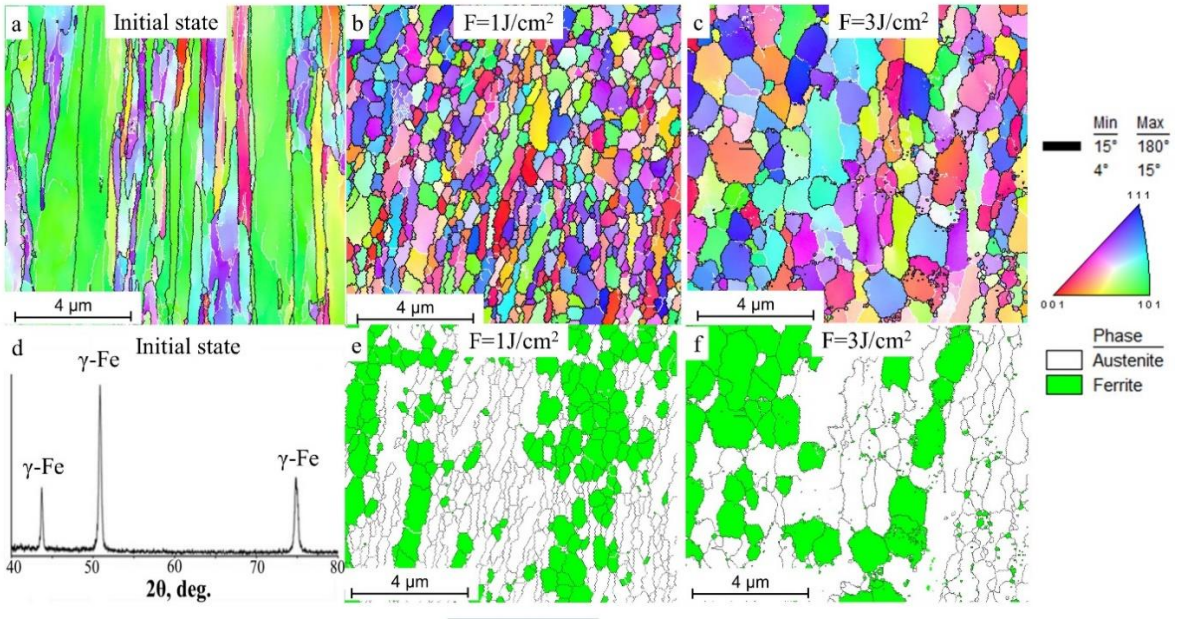

Figure 3. Microstructure and phase composition of AISI 321 steel before (a, d) and after HPIB processing at F = 1 J/cm^2 (b, e) and F = 3 J/cm^2 (c, f). OIM (a-c), phase distribution (e, f), EBSD maps, and XRD pattern (d).

In the initial state, the steel exhibits a single austenite (fcc) phase structure (Figure 3d). Ion irradiation promotes the formation of the ferrite (bcc) phase that coexists with the fcc phase (Figure 3e,f). According to the EBSD data, the fraction of ferrite is 35% for F = 1 J/cm^2 and 23% for F = 3 J/cm^2.

3.3. Corrosion properties

The DL-EPR polarization curves for AISI 321 stainless steel are shown in Figure 4. The current density of the first (passivation) peak increases after ion beam processing (No.1-3 in Figure 4a). The increase in the current density indicates more intense dissolution. This can be attributed to the formation of a secondary phase (ferrite) in the near-surface layers after irradiation. Simultaneously, the intensity of the reverse (reactivation) peak decreases compared with that of the peak of the original untreated surface (No.1-3 in Figure 4b). This may be associated with the redistribution of chromium due to HPIB processing, which facilitates the formation of a more stable protective oxide film on the steel surface.

The degree of sensitization is characterized by the reactivation coefficient R_r; it is the ratio of the areas of the reactivation peak (Figure 4b) to the passivation peak (Figure 4a). According to the method used, the steel with a R_r of less than 0.11 is resistant to intergranular corrosion. The smaller the R_r value, the greater the intergranular corrosion resistance. The original state with the R_r = 0.06 is resistant to intergranular corrosion, as can be observed from Figure 4c. R_r decreased to 0.009 after HPIB processing with F = 1 J/cm^2. The steel had the same resistance to intergranular corrosion (R_r = 0.007) as the coarse-grained austenitic structure after processing with F = 3 J/cm^2.

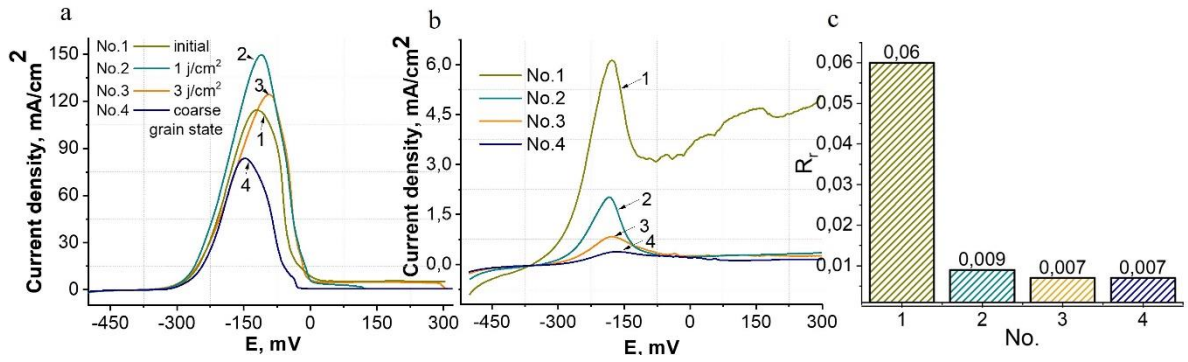

Figure 4. Potentiodynamic polarization curves [forward (a) and reverse (b)] and reactivation ratios (c) of AISI 321 stainless steel before and after HPIB processing.

4. Conclusion

1. The surface irradiation of AISI 321 stainless steel by a high-power ion beam leads to surface defects in the form of rounded craters. It was demonstrated that inclusions based on Ti and S are the preferred sites for crater formation.
2. HPIB processing of AISI 321 stainless steel causes a variation in the structure of the surface layers, involving the formation of microstructure grains that are more uniform in size. This results in a high degree of equiaxiality and an increased fraction of high-angle grain boundaries in the modified layer.
3. The resistance of steel to intergranular corrosion improves significantly after HPIB processing.

Acknowledgments

The reported study was funded by RFBR, project number 20-08-00907.

References

[1] Korotaev A D, Tyumentsev A N, Pinzhin Yu P, Remnev G E, 2004 Surface & Coatings Technology **185** 38–49
[2] Shulov V A, Nochovnaya N A, Remnev G E, 1998 Materials Science and Engineering A **243** 290 –3
[3] Ma X, Zhang G, Wang G, Zhu G, Zhou W, Wang J, Sun B, 2014 Applied Surface Science **311** 567-73
[4] Wang X, Lei M K, Zhang J S, 2007 Surface & Coatings Technology **201** 5884–90
[5] Zhong H, Zhang J, Shen J, Yu X, Liang G, Cui X, Zhang X, Zhang G, Yan S, Le X, 2017 Nuclear Instruments and Methods in Physics Research B **409** 298-301
[6] Zhong H, Zhang J, Shen J, Liang G, Zhang Sh, Xu M, Yu X, Yan S, Remnev G E, Le X, 2020 Vacuum **179** 109541
[7] Wang X, Han X G, Lei M K, Zhang J S, 2007 Materials Science and Engineering A **457** 84–89
[8] Remnev G E, Shulov V A 1993 Laser and Particle Beams **11** 707–731
[9] Wilson P R and Chen Z, 2007 Scripta Materialia **56** 753–756